DOI: 10.2478/aucts-2018-0008

ACTA UNIVERSITATIS CIBINIENSIS – TECHNICAL SERIES
Vol. LXX 2018

FLOW ANALYSIS OF POWELL-EYRING FLUID OVER AN OFF-CENTERED POROUS ROTATING DISK

Najeeb Alam Khan, Sidra Khan
Department of Mathematics, University of Karachi, Karachi 75270, Pakistan, njbalam@yahoo.com

Abstract: *This article presents the study of three-dimensional, stagnation flow of a Powell-Eyring fluid towards an off-centered rotating porous disk. A uniform injection or suction is applied through the surface of the disk. The Darcy law of porous disk for Powell-Eyring fluid is also obtained. The governing partial differential equations and their related boundary conditions are converted into ordinary differential equations by using a suitable similarity transformation. The analytical solution, of the system of equations is solved by using homotopy analysis method. The convergence region of the obtained solution is determined and plotted. The effects of rotational parameter, porosity of the medium, the characteristics of the non-Newtonian fluid and the suction or injection velocity on the velocity distributions is shown by graphical representation.*

Key words: Powell-Eyring fluid; porous disk; homotopy analysis method; Darcy's law

1. Introduction

The non-Newtonian fluids attracted the attention of researchers due to its applications in industries and engineering. The work in non-Newtonian fluid increased during the past few years. The constitutive equations of non-Newtonian fluids are more complicated and higher
order because of nonlinear relationship between stress and strain. Examples of such fluids include slurries, shampoo, printer ink, gum solutions, nail polish, whipped cream, toothpaste, grease, cosmetic products, custard, butter, blood plasma and many others. Hence much attention has been devoted to study the different models of non-Newtonian fluids. Powell-Eyring fluid model [1-5], a complex mathematical model developed by Powell and Eyring in 1944. One of the interesting features of Powell-Eyring fluids is that, the stress constitutive relation of such fluids can be derived using the kinetic theory of liquids. This model correctly reduces to Newtonian behavior for low and high shear rates [6]. Islam et al. [7] calculated the slider bearing lubricated of Powell-Eyring fluid by homotopy perturbation analysis method. Zueco et al. [8] studied the numerical effect of pulsatile flow of Powell-Eyring model and Patel et al. [9] examined the numerical solution of Powell-Eyring model past a wedge. Javed et al. [10] observed the effect of boundary layer flow of Powell-Eyring fluid over a stretching sheet. Akbar et al. [11] studied the Powell-Eyring peristaltic fluid flow with mass and heat transfer. Hayat et al. [12] investigated the flow and heat transfer of Powell-Eyring fluid over a continuously moving surface in the presence of a free stream velocity.
The fluid flow over an infinite rotating disk was first studied by Von-Karman [13] which then have got so much importance due to its significant applications in many industrial and engineering fields, for example spin-coating, computer storage devices, rotational viscometer, centrifugal machinery, pumping of liquid metals at high melting point, crystal growth from molten silicon, turbo machinery and most importantly aerodynamic applications. Millsaps [14] studied the heat transfer by laminar flow from a rotating disk. Ahmadpour and Sadeghy [15] investigated the Swirling flow of Bingham fluids above a rotating disk. Rashidi and Shahmohamadi [16] calculated the analytical solution of three dimensional Navier-Strokes equation for the flow near an infinite rotating disk. The problem of MHD flow of Powell-Eyring fluid over an infinite rotating disk under the presence of magnetic were found by Khan et al. [17]. The unsteady ferro fluid flow due to a rotating disk was considered between highly oscillating magnetic field and magnetization, the effect of higher angular frequency negative the rotational viscosity resulting in faster convergence of velocity components as compared to the ordinary case where rotational viscosity is zero was founded by Ram and Bhandari [18].

The non-alignment in the flow and disk axis makes it momentous to study the complex flow pattern of the fluid over rotating disk. The model of a stagnation point flow towards an off centered rotating disk was first proposed by Wang [19]. Dinarvand [20] calculated the analytic solutions of problem [20] by homotopy analysis method, he noticed that the performance of HAM solution for velocity functions shows the good agreement with the pervious study. Erfani and Rashidi [21] calculated the solution of stagnation flow toward an off-centered rotating disk by using the DTM–Padé technique, which is the combination of the differential transform and Padé approximation method. Nourbakhsh et al. [22] re-examined the analytical solution for off-centered stagnation flow towards a rotating disk by applying a semi-exact method with two auxiliary parameters to obtain the solution, numerical computation has also been made for the verification of the study. Khan et al. [23-24] extended the work of Wang [19] by finding the analytical solutions of non-Newtonian fluids like Jeffery and couple stress fluid.

In all the articles highlighted above, porous medium was not taken into account. The non-Newtonian study through a porous medium is an interesting topic these days, especially with the introduction of the modified Darcy's law. Flow through a porous medium has practical applications, especially in geophysical fluid dynamics. Some of the examples of natural porous media are limestone, beach sand, the human lung, sandstone, wood, rye bread, bile duct, small blood vessels and gall bladder with stones. Number of researchers employing Darcy's law, recently, Shahzad et al. [25] investigated the effect of porous half space on forth order fluid, also the modified Darcy's law is considered and its flow characteristics are also taken into account. Tan and Masuoka [26-27] extended the Stokes's first problem on the bases of modified Darcy's law for the second grade and Oldroyd-B fluid in a porous half space with a heated flat plate. Hayat et al. [28] calculated the MHD flow of a non Newtonian Maxwell fluid which is constructed in a rotating frame through a porous medium. Attia [29-30] investigated the viscous non-Newtonian fluid above an infinite rotating porous disk in a porous medium with heat transfer, a uniform injection /suction is applied through the surface of the disk and he also studied the unsteady flow and heat transfer of viscous fluid with temperature-dependent viscosity due to a rotating disk in a porous medium.

The objective of this present study is to explore the effect of three dimensional non Newtonian Powell- Eyring fluids at stagnation point towards an off-centered rotating porous disk. A uniform suction or injection is applied through the surface of the porous disk. The expression for Darcy resistance of Powell-Eyring fluid is also obtained. The ordinary differential equations (ODEs) are solved by non perturbation technique HAM. The influence of fluid parameters, rotating disk parameter porosity and permeability of the porous medium on the velocity functions are presented in graphical form.

2. Basic Equations

The flow is governed by the continuity and momentum equation in the forms

$$\nabla.\boldsymbol{V} = 0 \tag{1}$$

$$\rho(\boldsymbol{V}.\nabla)\boldsymbol{V} = -\nabla p + \nabla.\boldsymbol{S} + \boldsymbol{R} \tag{2}$$

$$\boldsymbol{S} = \left\{\mu + \frac{1}{\beta\,\dot{\gamma}}\sinh^{-1}\left(\frac{1}{c}\dot{\gamma}\right)\right\}\left(\nabla\boldsymbol{V} + \nabla\boldsymbol{V}^{T}\right) \tag{3}$$

Where

$$\left|\bar{\dot{\gamma}}\right| = \sqrt{\frac{1}{2}tr(\nabla\boldsymbol{V} + \nabla\boldsymbol{V}^{T})^{2}} \tag{4}$$

Where $\boldsymbol{V}$ is the velocity, ρ is the fluid density, μ is the dynamic viscosity of the fluid, $\boldsymbol{S}$ is the extra stress tensor, β and c are the fluid parameters of the Eyring-Powell fluid, c has the dimension of $(time)^{-1}$ and $\boldsymbol{R}$ is the Darcy resistance. We take the second-order approximation of $\sinh^{-1}$ function as

$$\sinh^{-1}\left(\frac{1}{c}\dot{\gamma}\right) \cong \frac{\dot{\gamma}}{c} - \frac{\dot{\gamma}^{3}}{6c^{3}}, \qquad \text{with} \quad \frac{\dot{\gamma}^{5}}{c^{5}} << 1 \tag{5}$$

The three scalar momentum equations are

$$\left((V.\nabla)V\right)_{x} = -\frac{\partial p}{\partial x} + \frac{\partial S_{xx}}{\partial x} + \frac{\partial S_{xy}}{\partial y} + \frac{\partial S_{xz}}{\partial z} + R_{x} \tag{6}$$

$$\left((V.\nabla)V\right)_y = -\frac{\partial p}{\partial y} + \frac{\partial S_{yx}}{\partial x} + \frac{\partial S_{yy}}{\partial y} + \frac{\partial S_{yz}}{\partial z} + R_y \tag{7}$$

$$\left((V.\nabla)V\right)_z = -\frac{\partial p}{\partial z} + \frac{\partial S_{zx}}{\partial x} + \frac{\partial S_{zy}}{\partial y} + \frac{\partial S_{zz}}{\partial z} + R_z \tag{8}$$

In Eqs. (6)- (8) the subscripts x,y and z indicate the components in the x-,y - and z - directions. Whereas R_x, R_y and R_z are the x-,y - and z - components of the Darcy's resistance R.

3. Problem Formulation

Let us assume the steady three-dimensional rotational flow of an incompressible Powell- Eyring fluid at stagnation point flow over an off-centered rotating porous disk. The flow axis of this disk is parallel to z axis at a distance s. The radius of disk is infinite, and it is moving with an angular velocity Ω in a porous medium. A uniform injection or suction is applied at the surface of the disk for the entire range from large injection velocities to large suction velocities. Let u,v and w are the velocity components along x, y and z directions, respectively. The stress tensor in an Eyring-Powell fluid is given by (Powell and Eyring, 1944; Steffe, 1996). The geometry of the problem is presented below in Fig.1

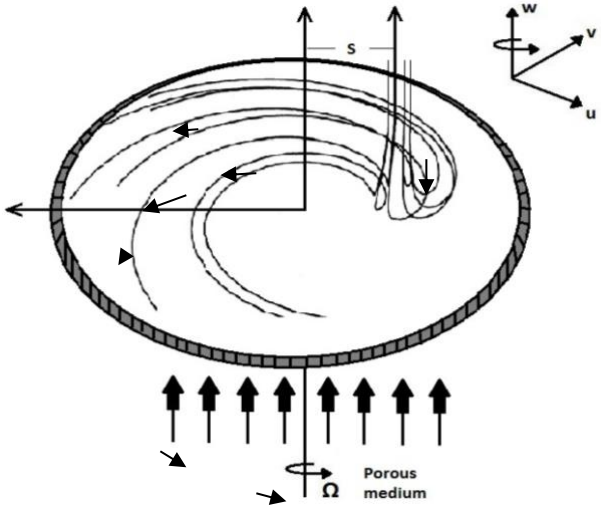

Fig 1. Geometry of the Problem.

The three scalar momentum equations are of Eyring-Powell fluid is expressed as follows:

$$\frac{\partial u}{\partial x} + \frac{\partial v}{\partial y} + \frac{\partial w}{\partial z} = 0 \tag{9}$$

$$u\frac{\partial u}{\partial x}+v\frac{\partial u}{\partial y}+w\frac{\partial u}{\partial z}=-\frac{1}{\rho}\frac{\partial p}{\partial x}+\left(\nu+\frac{1}{\rho\beta c}\right)\left[\frac{\partial^2 u}{\partial x^2}+\frac{\partial^2 u}{\partial y^2}+\frac{\partial^2 u}{\partial z^2}\right]$$
$$-\frac{1}{3\rho\beta c^3}\frac{\partial}{\partial x}\left\{2\left(\frac{\partial u}{\partial x}\right)^2+2\left(\frac{\partial v}{\partial y}\right)^2+2\left(\frac{\partial w}{\partial z}\right)^2+\left(\frac{\partial u}{\partial y}+\frac{\partial v}{\partial x}\right)^2+\left(\frac{\partial u}{\partial z}+\frac{\partial w}{\partial x}\right)^2+\left(\frac{\partial v}{\partial z}+\frac{\partial w}{\partial y}\right)^2\right\}\left(\frac{\partial u}{\partial x}\right)$$
$$-\frac{1}{6\rho\beta c^3}\frac{\partial}{\partial y}\left\{2\left(\frac{\partial u}{\partial x}\right)^2+2\left(\frac{\partial v}{\partial y}\right)^2+2\left(\frac{\partial w}{\partial z}\right)^2+\left(\frac{\partial u}{\partial y}+\frac{\partial v}{\partial x}\right)^2+\left(\frac{\partial u}{\partial z}+\frac{\partial w}{\partial x}\right)^2+\left(\frac{\partial v}{\partial z}+\frac{\partial w}{\partial y}\right)^2\right\}\left(\frac{\partial u}{\partial y}+\frac{\partial v}{\partial x}\right)$$
$$-\frac{1}{6\rho\beta c^3}\frac{\partial}{\partial z}\left\{2\left(\frac{\partial u}{\partial x}\right)^2+2\left(\frac{\partial v}{\partial y}\right)^2+2\left(\frac{\partial w}{\partial z}\right)^2+\left(\frac{\partial u}{\partial y}+\frac{\partial v}{\partial x}\right)^2+\left(\frac{\partial u}{\partial z}+\frac{\partial w}{\partial x}\right)^2+\left(\frac{\partial v}{\partial z}+\frac{\partial w}{\partial y}\right)^2\right\}\left(\frac{\partial u}{\partial z}+\frac{\partial w}{\partial x}\right)$$
$$-\frac{\phi}{k_1}\left(\left(\mu+\frac{1}{\beta c}\right)-\frac{1}{6\rho\beta c^3}\left(2\left(\frac{\partial u}{\partial x}\right)^2+2\left(\frac{\partial v}{\partial y}\right)^2+2\left(\frac{\partial w}{\partial z}\right)^2+\left(\frac{\partial u}{\partial y}+\frac{\partial v}{\partial x}\right)^2+\left(\frac{\partial u}{\partial z}\right)^2+\left(\frac{\partial v}{\partial z}\right)^2\right)\right)u \quad (10)$$

$$u\frac{\partial v}{\partial x}+v\frac{\partial v}{\partial y}+w\frac{\partial v}{\partial z}=-\frac{1}{\rho}\frac{\partial p}{\partial y}+\left(\nu+\frac{1}{\rho\beta c}\right)\left[\frac{\partial^2 v}{\partial x^2}+\frac{\partial^2 v}{\partial y^2}+\frac{\partial^2 v}{\partial z^2}\right]$$
$$-\frac{1}{6\rho\beta c^3}\frac{\partial}{\partial x}\left\{2\left(\frac{\partial u}{\partial x}\right)^2+2\left(\frac{\partial v}{\partial y}\right)^2+2\left(\frac{\partial w}{\partial z}\right)^2+\left(\frac{\partial u}{\partial y}+\frac{\partial v}{\partial x}\right)^2+\left(\frac{\partial u}{\partial z}+\frac{\partial w}{\partial x}\right)^2+\left(\frac{\partial v}{\partial z}+\frac{\partial w}{\partial y}\right)^2\right\}\left(\frac{\partial u}{\partial y}+\frac{\partial v}{\partial x}\right)$$
$$-\frac{1}{3\rho\beta c^3}\frac{\partial}{\partial y}\left\{2\left(\frac{\partial u}{\partial x}\right)^2+2\left(\frac{\partial v}{\partial y}\right)^2+2\left(\frac{\partial w}{\partial z}\right)^2+\left(\frac{\partial u}{\partial y}+\frac{\partial v}{\partial x}\right)^2+\left(\frac{\partial u}{\partial z}+\frac{\partial w}{\partial x}\right)^2+\left(\frac{\partial v}{\partial z}+\frac{\partial w}{\partial y}\right)^2\right\}\left(\frac{\partial v}{\partial y}\right)$$
$$-\frac{1}{6\rho\beta c^3}\frac{\partial}{\partial z}\left\{2\left(\frac{\partial u}{\partial x}\right)^2+2\left(\frac{\partial v}{\partial y}\right)^2+2\left(\frac{\partial w}{\partial z}\right)^2+\left(\frac{\partial u}{\partial y}+\frac{\partial v}{\partial x}\right)^2+\left(\frac{\partial u}{\partial z}+\frac{\partial w}{\partial x}\right)^2+\left(\frac{\partial v}{\partial z}+\frac{\partial w}{\partial y}\right)^2\right\}\left(\frac{\partial v}{\partial z}+\frac{\partial w}{\partial y}\right)$$
$$-\frac{\phi}{k_1}\left(\left(\mu+\frac{1}{\beta c}\right)-\frac{1}{6\rho\beta c^3}\left(2\left(\frac{\partial u}{\partial x}\right)^2+2\left(\frac{\partial v}{\partial y}\right)^2+2\left(\frac{\partial w}{\partial z}\right)^2+\left(\frac{\partial u}{\partial y}+\frac{\partial v}{\partial x}\right)^2+\left(\frac{\partial u}{\partial z}\right)^2+\left(\frac{\partial v}{\partial z}\right)^2\right)\right)v \quad (11)$$

$$u\frac{\partial w}{\partial x}+v\frac{\partial w}{\partial y}+w\frac{\partial w}{\partial z}=-\frac{1}{\rho}\frac{\partial p}{\partial z}+\left(\nu+\frac{1}{\rho\beta c}\right)\left[\frac{\partial^2 w}{\partial x^2}+\frac{\partial^2 w}{\partial y^2}+\frac{\partial^2 w}{\partial z^2}\right]$$
$$-\frac{1}{6\rho\beta c^3}\frac{\partial}{\partial x}\left\{2\left(\frac{\partial u}{\partial x}\right)^2+2\left(\frac{\partial v}{\partial y}\right)^2+2\left(\frac{\partial w}{\partial z}\right)^2+\left(\frac{\partial u}{\partial y}+\frac{\partial v}{\partial x}\right)^2+\left(\frac{\partial u}{\partial z}+\frac{\partial w}{\partial x}\right)^2+\left(\frac{\partial v}{\partial z}+\frac{\partial w}{\partial y}\right)^2\right\}\left(\frac{\partial u}{\partial z}+\frac{\partial w}{\partial x}\right)$$
$$-\frac{1}{6\rho\beta c^3}\frac{\partial}{\partial y}\left\{2\left(\frac{\partial u}{\partial x}\right)^2+2\left(\frac{\partial v}{\partial y}\right)^2+2\left(\frac{\partial w}{\partial z}\right)^2+\left(\frac{\partial u}{\partial y}+\frac{\partial v}{\partial x}\right)^2+\left(\frac{\partial u}{\partial z}+\frac{\partial w}{\partial x}\right)^2+\left(\frac{\partial v}{\partial z}+\frac{\partial w}{\partial y}\right)^2\right\}\left(\frac{\partial w}{\partial y}+\frac{\partial v}{\partial z}\right) \quad (12)$$
$$-\frac{1}{3\rho\beta c^3}\frac{\partial}{\partial z}\left\{2\left(\frac{\partial u}{\partial x}\right)^2+2\left(\frac{\partial v}{\partial y}\right)^2+2\left(\frac{\partial w}{\partial z}\right)^2+\left(\frac{\partial u}{\partial y}+\frac{\partial v}{\partial x}\right)^2+\left(\frac{\partial u}{\partial z}+\frac{\partial w}{\partial x}\right)^2+\left(\frac{\partial v}{\partial z}+\frac{\partial w}{\partial y}\right)^2\right\}\left(\frac{\partial w}{\partial z}\right)$$
$$-\frac{\phi}{k_1}\left(\left(\mu+\frac{1}{\beta c}\right)-\frac{1}{6\rho\beta c^3}\left(2\left(\frac{\partial w}{\partial z}\right)^2\right)\right)w$$

where $\nu=\frac{\mu}{\rho}$ is the kinematic viscosity. The boundary conditions near the disk and far from the disk are

$$u = -\Omega\, y, \qquad v = \Omega(x - s), \qquad w = w_0, \tag{13}$$

$$u = a\, x, \qquad v = a\, y, \qquad w = -2a\, z, \tag{14}$$

where a represents the strength of the stagnation flow. The similarity transformations presented by Wang [19] are

$$u = axf'(\eta) - \Omega y g(\eta) + s\,\Omega\, k(\eta),$$
$$v = ayf'(\eta) + \Omega x g(\eta) + s\Omega h(\eta),$$
$$w = -2\sqrt{a\nu}\, f(\eta), \quad \eta = z\sqrt{a/\nu} \tag{15}$$

Using the similarity transformations of Eq.(15) in Eqs. (9)-(12), the continuity equation satisfied whereas the governing partial differential equations are reduced to the following form:

$$(1+\lambda) f''' - (1+\lambda) M\, f' + \begin{pmatrix} 1 + 2ff'' - f'^2 \\ + \alpha^2 g^2 \end{pmatrix} - \lambda \begin{pmatrix} \xi^2 \begin{pmatrix} \frac{2}{3}\alpha^2 f' g'^2 + \frac{14}{3} f'\, f''^2 \\ + 2 f'^2 f''' - 2M\, f'^3 \end{pmatrix} \\ + \gamma \begin{pmatrix} + \alpha\, h' k' g'' + \alpha\, g' k' h'' \\ + h'\, f'' h'' + \alpha\, g' h' k'' + k'\, f'' k'' \\ + \frac{1}{2} h'^2\, f''' + \frac{3}{2} k'^2 f''' - M\alpha\, k\, g' h' \\ - \frac{M}{2} h'^2\, f' - \frac{M}{2} k'^2\, f' - M\, k'\, f'' k \end{pmatrix} \end{pmatrix} = 0, \tag{16}$$

$$(1+\lambda) g'' - (1+\lambda) M g + (2 f\, g' - 2 g\, f') - \lambda \begin{pmatrix} \xi^2 \left(4 f' g' f'' + 2 f'^2 g'' - 2M\, g\, f'^2\right) \\ + \gamma \begin{pmatrix} \frac{3}{2} h'^2 g'' + \frac{1}{2} k'^2 g'' + 3 g' h' h'' + g' k' k'' \\ + \frac{1}{\alpha} k' f' h'' + \frac{1}{\alpha} h' f' k'' + \frac{1}{\alpha} h' k' f''' \\ - M\, g' h' h - \frac{M}{2} h'^2 g - \frac{M}{2} k'^2 g - \frac{M}{\alpha} h k\, f'' \end{pmatrix} \end{pmatrix} = 0, \tag{17}$$

$$(1+\lambda) k'' - (1+\lambda) M\, k + (2 f\, k' - k\, f' + \alpha\, h\, g) - \lambda \begin{pmatrix} \xi^2 \begin{pmatrix} \frac{2}{3}\alpha\, g' h'\, f' + \frac{14}{3} f' k'\, f'' \\ + 2 f'^2\, k'' - 2M\, f'^2 k \end{pmatrix} \\ + \gamma \begin{pmatrix} h' k' h'' + \frac{1}{2} h'^2\, k'' + \frac{3}{2}\, k'^2\, k'' \\ - \frac{M}{2}\, k'^2 k - \frac{M}{2}\, h'^2 k \end{pmatrix} \end{pmatrix} = 0, \tag{18}$$

$$(1+\lambda)h''-(1+\lambda)M\ h+(2f\,h'-h\,f'-\alpha\ g\ k)-\lambda\left(\begin{array}{l}\xi^2\left(\begin{array}{l}+\frac{14}{3}f'\,h'\,f''-\frac{2}{3}\alpha\ g'\ f'\,k'\\+2\ f'^2\ h''-2M\ f'^2k\end{array}\right)\\+\gamma\left(\begin{array}{l}\frac{3}{2}h''\,h'^2+\frac{1}{2}k'^2\ h''+h'\,k'\,k''\\-\frac{M}{2}k'^2\ k-\frac{M}{2}h'^2\ k\end{array}\right)\end{array}\right)=0. \tag{19}$$

And the boundary conditions transformed to:

$$\begin{array}{llll} f(0)=V_0, & f'(0)=0, & g(0)=1, & k(0)=0, \quad h(0)=1, \\ f'(\infty)=1, & g(\infty)=0, & k(\infty)=0, & h(\infty)=0 \end{array} \tag{20}$$

where $\alpha=\frac{\Omega}{a}$ is the non-dimensional rotational parameter $\gamma=\frac{ab^2\Omega^2}{3c^2\nu}$, $\lambda=\frac{1}{c\beta\mu}$, and $\xi=\frac{a}{c}$ are the fluid parameters $M=\frac{\nu\,\phi}{a\,k_1}$ is the porosity parameter, $V_0=\frac{-w_0}{2\sqrt{a\nu}}$ is the uniform suction/injection parameter, and primes denote the differentiation with respect to η. The pressure p can be recovered by

$$\begin{aligned} p=p_0-\frac{1}{2}\rho\left(a^2\left(x^2+y^2\right)+w^2\right)+\left(\mu+\frac{1}{\beta c}\right)w_z-\frac{1}{6\beta c^3}\left(\frac{8w_z^{\,3}}{3}\right) \\ -\frac{\phi}{k_1}\int\left(\left(\mu+\frac{1}{\beta c}\right)w-\frac{1}{6\rho\beta\ c^3}\left(2\left(\frac{\partial w}{\partial z}\right)^2\right)w\right)dz, \end{aligned} \tag{21}$$

where p_0 is the pressure at the origin and ρ is the fluid density. The shear stress of the Powell- Eyring fluid on off centered rotating disk is given as follows

$$S_x=\rho\left(\nu+\frac{1}{\rho\beta\,c}\right)\left(\frac{\partial u}{\partial z}+\frac{\partial w}{\partial x}\right)-\frac{1}{6\rho\beta\,c^3}\left(\begin{array}{l}2\left(\frac{\partial u}{\partial x}\right)^2+2\left(\frac{\partial v}{\partial y}\right)^2+2\left(\frac{\partial w}{\partial z}\right)^2\\+\left(\frac{\partial u}{\partial y}+\frac{\partial v}{\partial x}\right)^2+\left(\frac{\partial u}{\partial z}+\frac{\partial w}{\partial x}\right)^2+\left(\frac{\partial v}{\partial z}+\frac{\partial w}{\partial y}\right)^2\end{array}\right)\left(\frac{\partial u}{\partial z}+\frac{\partial w}{\partial x}\right)\Bigg|_{z=0} \tag{22}$$

$$S_y=\rho\left(\nu+\frac{1}{\rho\beta\,c}\right)\left(\frac{\partial v}{\partial z}+\frac{\partial w}{\partial y}\right)-\frac{1}{6\rho\beta\,c^3}\left(\begin{array}{l}2\left(\frac{\partial u}{\partial x}\right)^2+2\left(\frac{\partial v}{\partial y}\right)^2+2\left(\frac{\partial w}{\partial z}\right)^2\\+\left(\frac{\partial u}{\partial y}+\frac{\partial v}{\partial x}\right)^2+\left(\frac{\partial u}{\partial z}+\frac{\partial w}{\partial x}\right)^2+\left(\frac{\partial v}{\partial z}+\frac{\partial w}{\partial y}\right)^2\end{array}\right)\left(\frac{\partial v}{\partial z}+\frac{\partial w}{\partial y}\right)\Bigg|_{z=0} \tag{23}$$

$$S_x = \rho a\sqrt{\nu a}\left[\begin{array}{l} x\left(f''(0)+\lambda f''(0)-2\lambda\xi^2 f'^2(0)f''(0)-\frac{3}{2}\lambda\gamma k'^2(0)f''(0)-\lambda\gamma\alpha g'(0)k'(0)h'(0)-\frac{1}{2}\lambda\gamma h'^2(0)f''(0)\right) \\ -\alpha y\left(g'(0)+\lambda g'(0)-2\lambda\xi^2 f'^2(0)g'(0)-\frac{3}{2}\lambda\gamma\beta g'(0)k'^2(0)-\frac{1}{2}\lambda\gamma g'(0)h'^2(0)-\frac{1}{\alpha}\lambda\gamma h'(0)k'(0)f''(0)\right) \\ -\frac{x^2}{2b}\left(\lambda\gamma\alpha g'^2(0)k'(0)+2\lambda\gamma g'(0)f''(0)h'(0)+\frac{3}{\alpha}\lambda\gamma k'(0)f''^2(0)\right) \\ -\frac{y^2}{2b}\left(3\lambda\gamma\alpha g'^2(0)k'(0)-2\lambda\gamma g'(0)f''(0)h'(0)+\frac{1}{\alpha}\lambda\gamma k'(0)f''^2(0)\right) \\ +\frac{x^2y}{2b^2}\left(\lambda\gamma\alpha g'^3(0)+\frac{1}{\alpha}\lambda\gamma g'(0)f''^2(0)\right)-\frac{xy^2}{2b^2}\left(\lambda\gamma g'^2(0)f''(0)+\frac{1}{\alpha^2}\lambda\gamma f''^3(0)\right) \\ -\frac{x^3}{2b^2}\left(\lambda\gamma g'^2(0)f''(0)+\frac{1}{\alpha^2}\lambda\gamma f''^3(0)\right)+\frac{y^3}{2b^2}\left(\lambda\gamma\alpha f'^3(0)+\frac{1}{\alpha}\lambda\gamma g'(0)f''^2(0)\right) \\ +\frac{xy}{b}\left(\lambda\gamma\alpha g'^2(0)h'(0)+2\lambda\gamma g'(0)f''(0)k'(0)-\frac{1}{\alpha}\lambda\gamma h'(0)f''^2(0)\right) \\ +b\alpha\left(k'(0)+\lambda k'(0)-\frac{6}{b}a\lambda\nu\gamma f'^2(0)k'(0)-\frac{1}{2}\lambda\gamma h'^2(0)k'(0)-\frac{1}{2}\lambda\gamma k'^3(0)\right) \end{array}\right] \quad (24)$$

$$S_y = \rho a\sqrt{\nu a}\left[\begin{array}{l} x\alpha\left(g'(0)+\lambda g'(0)-2\lambda\xi^2 f'^2(0)g'(0)-\frac{3}{2}\lambda\gamma g'(0)h'^2(0)-\frac{1}{2}\lambda\gamma g'(0)k'^2(0)-\frac{1}{\alpha}\lambda\gamma h'(0)k'(0)f''(0)\right) \\ -y\left(g'(0)+\lambda g'(0)-2\lambda\xi^2 f'^2(0)g'(0)-\frac{3}{2}\lambda\gamma g'(0)k'^2(0)-\frac{1}{2}\lambda\gamma g'(0)h'^2(0)-\frac{1}{\alpha}\lambda\gamma h'(0)k'(0)f''(0)\right) \\ -\frac{x^2}{2b}\left(\lambda\gamma\alpha g'^2(0)k'(0)+2\lambda\gamma g'(0)f''(0)h'(0)+\frac{3}{\alpha}\lambda\gamma k'(0)f''^2(0)\right) \\ -\frac{y^2}{2b}\left(3\lambda\gamma\alpha g'^2(0)k'(0)-2\lambda\gamma g'(0)f''(0)h'(0)+\frac{1}{\alpha}\lambda\gamma k'(0)f''^2(0)\right) \\ +\frac{x^2y}{2b^2}\left(\lambda\gamma\alpha g'^3(0)+\frac{1}{\alpha}\lambda\gamma g'(0)f''^2(0)\right)-\frac{xy^2}{2b^2}\left(\lambda\gamma g'^2(0)f''(0)+\frac{1}{\alpha^2}\lambda\gamma f''^3(0)\right) \\ -\frac{x^3}{2b^2}\left(\lambda\gamma g'^2(0)f''(0)+\frac{1}{\alpha^2}\lambda\gamma f''^3(0)\right)+\frac{y^3}{2b^2}\left(\lambda\gamma\alpha f'^3(0)+\frac{1}{\alpha}\lambda\gamma g'(0)f''^2(0)\right) \\ +\frac{xy}{b}\left(\lambda\gamma\alpha g'^2(0)h'(0)+2\lambda\gamma g'(0)f''(0)k'(0)-\frac{1}{\alpha}\lambda\gamma h'(0)f''^2(0)\right) \\ +b\alpha\left(k'(0)+\lambda k'(0)-\frac{6}{b}a\lambda\nu\gamma f'^2(0)k'(0)-\frac{1}{2}\lambda\gamma h'^2(0)k'(0)-\frac{1}{2}\lambda\gamma k'^3(0)\right) \end{array}\right] \quad (25)$$

The shear stress at the center is zero, by solving Eq. (24)-(25) for (x,y) we can obtain the shear center on the surface of disk. The torque of the disk experienced by radius R is given as

$$T = \int_0^R\int_0^{2\pi}\left(S_y\cos\varphi - S_x\sin\varphi\right)r^2 d\varphi\, dr, \quad (26)$$

where (r,φ) are cylindrical coordinates. Since $x = r\,Cos\varphi - s$ and $y = r\,Sin\varphi$, the torque can be found as:

$$T = \frac{\pi}{2}a\sqrt{a\nu}\,\alpha R^4\,\rho\left(g'(0)+\lambda\left(\begin{array}{l} g'(0)-2\xi^2 f'^2(0)g'(0)-\gamma g'^3(0)+2\gamma g'^2(0)h'(0) \\ -\gamma g'(0)h'^2(0)-\gamma g'(0)k'^2(0)+\frac{2\gamma}{\alpha}g'(0)k'(0)f''(0) \\ \frac{\gamma}{\alpha^2}g'(0)f''^2(0)-\frac{R^2a\xi^2}{9\nu}\left(\alpha^2 g'^3(0)+g'(0)f''^2(0)\right) \end{array}\right)\right) \quad (27)$$

which remain unchange by the flow axis and non-aligned disk. The system of ordinary differential equations, of Powell-Eyring fluid is presented by Eqs. (16)-(19) are transformed into the Navier-Stokes equations of stagnation flow [19] by keeping the paramertes of Powell-Eyring fluid (λ, ξ and γ), porosity parameter (M) and Suction/Injection parameter V_0 equivalent to zero.

4. The HAM solution of the problem

For HAM solution, following initial guess of $f(\eta), g(\eta), k(\eta)$ and $h(\eta)$ has been selected:

$$\tilde{f}_0(\eta) = \eta + V_0 - 1 + e^{-\eta},\ \tilde{g}_0(\eta) = e^{-\eta},\ \tilde{k}_0(\eta) = \eta e^{-\eta},\ \tilde{h}_0(\eta) = e^{-\eta} \tag{28}$$

and choose the auxiliary linear operators:

$$L_1[f] = \frac{\partial^3}{\partial \eta^3} - \frac{\partial}{\partial \eta} \qquad L_2[g,k,h] = \frac{\partial^2}{\partial \eta^2} - 1 \tag{29}$$

such that

$$L_1\left(c_1 + c_2 e^{\eta} + c_3 e^{-\eta}\right) = 0, \qquad L_2\left(c_4 e^{\eta} + c_5 e^{-\eta}\right) = 0 \tag{30}$$

$c_i (i = 1,2,....5)$ are constants. The zeroth-order deformation, problem of non auxiliary parameters $\hbar_1, \hbar_2, \hbar_3$ and $\hbar_4$ are formulated below:

$$(1-p)L_1\left[\tilde{f}(\eta, p) - \tilde{f}_0(\eta)\right] = p\,\hbar_1 \mathrm{N}_1\left[\tilde{f}(\eta, p), \tilde{g}(\eta, p)\right] \tag{31}$$

$$(1-p)L_2\left[\tilde{g}(\eta, p) - \tilde{g}_0(\eta)\right] = p\,\hbar_2 \mathrm{N}_2\left[\tilde{f}(\eta,p), \tilde{g}(\eta,p)\right] \tag{32}$$

$$(1-p)L_2\left[\tilde{k}(\eta, p) - \tilde{k}_0(\eta)\right] = p\,\hbar_3 \mathrm{N}_3\left[\tilde{f}(\eta,p), \tilde{g}(\eta,p), \tilde{k}(\eta, p), \tilde{h}(\eta, p)\right] \tag{33}$$

$$(1-p)L_2\left[\tilde{h}(\eta, p) - \tilde{h}_0(\eta)\right] = p\,\hbar_4 \mathrm{N}_4\left[\tilde{f}(\eta,p), \tilde{g}(\eta,p), \tilde{k}(\eta, p), \tilde{h}(\eta,p)\right] \tag{34}$$

subjected to the boundary conditions

$$\tilde{f}(0;p) = V_0, \quad \tilde{f}'(0;p) = 0, \quad \tilde{f}'(\infty;p) = 1, \quad \tilde{g}(0;p) = 1, \quad \tilde{g}(\infty;p) = 0, \quad \tilde{k}(0;p) = 0,$$
$$\tilde{k}(\infty;p) = 0, \quad \tilde{h}(0;p) = 1, \quad \tilde{h}(\infty;p) = 0, \tag{35}$$

$p \in [0, 1]$ is the embedding paramerter and $\mathrm{N}_1, \mathrm{N}_2, \mathrm{N}_3$ and N_4 are the non-linear operators expressed as:

$$\mathrm{N}_1\left[f(\eta,p), g(\eta,p)\right] = (1+\lambda)f''' - (1+\lambda)M\ f' + \left(1 + 2ff'' - f'^2 + \alpha^2 g^2 - M\ f'\right)$$
$$-\lambda\left(\begin{array}{l} \xi^2\left(\frac{2}{3}\alpha^2 f'\, g'^2 + \frac{14}{3} f'\, f''^2 + 2f'^2 f''' - 2M\ f'^3\right) \\ +\gamma\left(\begin{array}{l} +\alpha\, h' k' g'' + \alpha\, g' k' h'' + h'\, f'' h'' + \alpha\, g' h' k'' \\ +k'\, f'' k'' + \frac{1}{2} h'^2\ f''' + \frac{3}{2} k'^2 f''' - M\, k'\, f'' k \\ -\frac{M}{2} h'^2\ f' - \frac{M}{2} k'^2\ f' - M\,\alpha\ k\, g' h' \end{array}\right) \end{array}\right) = 0, \tag{36}$$

$$\mathrm{N}_2[f(\eta,p),g(\eta,p)]=(1+\lambda)g''-(1+\lambda)Mg+(2f\ g'-2g\ f')$$
$$-\lambda\left(\begin{array}{l}\xi^2\left(4f'g'f''+2f'^2g''-2M\ g\ f'^2\right)\\ +\gamma\left(\begin{array}{l}\frac{3}{2}h'^2g''+\frac{1}{2}k'^2g''+3g'h'h''+g'k'k''\\ +\frac{1}{\alpha}k'f'h''+\frac{1}{\alpha}h'f'k''+\frac{1}{\alpha}h'k'f'''\\ -M\ g'h'\ h-\frac{M}{2}h'^2g-\frac{M}{2}k'^2g-\frac{M}{\alpha}h\ k\ f''\end{array}\right)\end{array}\right)=0, \tag{37}$$

$$\mathrm{N}_3[f(\eta,p),g(\eta,p),k(\eta,p),h(\eta,p)]=(1+\lambda)k''-(1+\lambda)M\ k+(2f\ k'-k\ f'+\alpha\ h\ g)$$
$$-\lambda\left(\begin{array}{l}\xi^2\left(\begin{array}{l}\frac{2}{3}\alpha\ g'\ h'\ f'+\frac{14}{3}\ f'\ k'\ f''\\ +2f'^2\ k''-2M\ f'^2k\end{array}\right)\\ +\gamma\left(\begin{array}{l}h'\ k'\ h''+\frac{1}{2}h'^2\ k''+\frac{3}{2}\ k'^2\ k''\\ -\frac{M}{2}\ k'^2k-\frac{M}{2}\ h'^2k\end{array}\right)\end{array}\right)=0, \tag{38}$$

$$\mathrm{N}_4[f(\eta,p),g(\eta,p),k(\eta,p),h(\eta,p)]=(1+\lambda)h''-(1+\lambda)M\ h+(2f\ h'-h\ f'-\alpha\ g\ k)$$
$$-\lambda\left(\begin{array}{l}\xi^2\left(\begin{array}{l}+\frac{14}{3}\ f'\ h'\ f''-\frac{2}{3}\alpha\ g'\ f'\ k'\\ +2\ f'^2\ h''-2M\ f'^2k\end{array}\right)\\ +\gamma\left(\begin{array}{l}\frac{3}{2}h''\ h'^2+\frac{1}{2}k'^2\ h''+h'\ k'\ k''\\ -\frac{M}{2}k'^2\ k-\frac{M}{2}h'^2\ k\end{array}\right)\end{array}\right)=0. \tag{39}$$

For $p=0$, we have the initial guess approximations

$$\tilde{f}(\eta;0)=\tilde{f}_0(\eta),\quad \tilde{g}(\eta;0)=\tilde{g}_0(\eta),\quad \tilde{k}(\eta;0)=\tilde{k}_0(\eta),\quad \tilde{h}(\eta;0)=\tilde{h}_0(\eta). \tag{40}$$

When $p=1$, the Eqs. (31)- (34) are similar as (16)-(19) respectively, so we obtain the final solutions at $p=1$

$$\tilde{f}(\eta;1)=\tilde{f}(\eta),\quad \tilde{g}(\eta;1)=\tilde{g}(\eta),\quad \tilde{k}(\eta;1)=\tilde{k}(\eta),\quad \tilde{h}(\eta;1)=\tilde{h}(\eta). \tag{41}$$

Hence the rise in p from 0 to 1 is the process of continuous variation of velocity functions $f(\eta;p),g(\eta;p),k(\eta;p)\text{and}\,h(\eta;p)$ from their initial guess $f_0(\eta),g_0(\eta)k_0(\eta)\text{amd}\,h_0(\eta)$ to the final solution $f(\eta),g(\eta)k(\eta)\text{amd}\,h(\eta)$. This type of continuous variation is known as deformation in topology so that we call the system of Eqs. (31)-(34), the zeroth order deformation equation. Next, the m^{th} - order deformation equations as follow

$$L_1[f_m(\eta)-\chi_m f_{m-1}(\eta)]=\hbar_1\ R_{1,m}(\eta) \tag{42}$$

$$L_2[g_m(\eta)-\chi_m g_{m-1}(\eta)]=\hbar_2\ R_{2,m}(\eta) \tag{43}$$

$$L_2\left[k_m(\eta)-\chi_m k_{m-1}(\eta)\right]=\hbar_3\, R_{3,m}(\eta) \tag{44}$$

$$L_2\left[h_m(\eta)-\chi_m h_{m-1}(\eta)\right]=\hbar_4\, R_{4,m}(\eta) \tag{45}$$

with the boundary conditions

$$f_m(0)=0,\quad f'_m(0)=0,\quad f'_m(\infty)=0,\quad g_m(0)=0,\quad g_m(\infty)=0,\quad k_m(0)=0,\quad k_m(\infty)=0,$$

$$h_m(0)=0,\quad h_m(\infty)=0 \tag{46}$$

Where

$$R_{1,m}(\eta)=f'''_{m-1}(\eta)(1+\lambda)-M\, f'_{m-1}(\eta)-\lambda M\, f'_{m-1}(\eta)+\sum_{i=0}^{m-1}\begin{pmatrix}-f_i'(\eta)f'_{m-1-i}(\eta)+\alpha^2\, g_i(\eta)g_{m-1-i}(\eta)\\+2f_i(\eta)f''_{m-1-i}(\eta)\end{pmatrix}$$

$$-\lambda\sum_{i=0}^{m-1}\left(\begin{array}{l}\xi^2\left(\begin{array}{l}\frac{2}{3}\alpha^2 f'_{m-1-i}(\eta)\sum_{j=0}^{i} g'_{i-j}(\eta)g'_j(\eta)+\frac{14}{3}f'_{m-1-i}(\eta)\sum_{j=0}^{i} f''_{i-j}(\eta)f''_j(\eta)\\+2f'''_{m-1-i}(\eta)\sum_{j=0}^{i} f'_{i-j}(\eta)f'_j(\eta)-2M\, f'_{m-1-i}(\eta)\sum_{j=0}^{i} f'_{i-j}(\eta)f'_j(\eta)\end{array}\right)\\ \gamma\left(\begin{array}{l}\alpha\, h'_{m-1-i}(\eta)\sum_{j=0}^{i} k'_{i-j}(\eta)g''_j(\eta)+\alpha\gamma\, g'_{m-1-i}(\eta)\sum_{j=0}^{i} k'_{i-j}(\eta)h''_j(\eta)\\+\alpha\, g'_{m-1-i}(\eta)\sum_{j=0}^{i} h'_{i-j}(\eta)k''_j(\eta)-M\alpha\, k_{m-1}(\eta)\sum_{j=0}^{i} g'_{i-j}(\eta)h'_j(\eta)\\+h'_{m-1-i}(\eta)\sum_{j=0}^{i} f''_{i-j}(\eta)h''_j(\eta)+k'_{m-1-i}(\eta)\sum_{j=0}^{i} f''_{i-j}(\eta)k''_j(\eta)\\+\frac{1}{2}f'''_{m-1-i}(\eta)\sum_{j=0}^{i} h'_{i-j}(\eta)h'_j(\eta)+\frac{3}{2}f'''_{m-1-i}(\eta)\sum_{j=0}^{i} k'_{i-j}(\eta)k'_j(\eta)\\-\frac{M}{2}f'_{m-1-i}(\eta)\sum_{j=0}^{i} h'_{i-j}(\eta)h'_j(\eta)-\frac{M}{2}f'_{m-1-i}(\eta)\sum_{j=0}^{i} k'_{i-j}(\eta)k'_j(\eta)\\-Mk'_{m-1-i}(\eta)\sum_{j=0}^{i} k_{i-j}(\eta)f_j''(\eta)\end{array}\right)\end{array}\right)+(1-\chi_m), \tag{47}$$

$$R_{2,m}(\eta)=g''_{m-1}(\eta)(1+\lambda)-Mg_{m-1}(\eta)-\lambda Mg_{m-1}(\eta)+\sum_{i=0}^{m-1}\left(2f_i(\eta)g'_{m-1-i}(\eta)-2g_i(\eta)f'_{m-1-i}(\eta)\right)$$

$$-\lambda\sum_{i=0}^{m-1}\left(\begin{array}{l}\xi^2\left(\begin{array}{l}4f'_{m-i-i}(\eta)\sum_{j=0}^{i}f''_{i-j}(\eta)g'_j(\eta)+2g''_{m-i-i}(\eta)\sum_{j=0}^{i}f'_{i-j}(\eta)f'_j(\eta)\\-2Mg_{m-i-i}(\eta)\sum_{j=0}^{i}f'_{i-j}(\eta)f'_j(\eta)\end{array}\right)\\+\gamma\left(\begin{array}{l}-M\ g'_{m-i-i}(\eta)\sum_{j=0}^{i}h'_{i-j}(\eta)h_j(\eta)-\frac{M}{2}h'_{m-i-i}(\eta)\sum_{j=0}^{i}h'_{i-j}(\eta)g_j(\eta)\\-\frac{M}{2}g_{m-i-i}(\eta)\sum_{j=0}^{i}k'_{i-j}(\eta)k'_j(\eta)\frac{3}{2}g''_{m-i-i}(\eta)\sum_{j=0}^{i}h'_{i-j}(\eta)h'_j(\eta)\\+\frac{1}{2}g''_{m-i-i}(\eta)\sum_{j=0}^{i}k'_{i-j}(\eta)k'_j(\eta)+3g'_{m-i-i}(\eta)\sum_{j=0}^{i}h'_{i-j}(\eta)h''_j(\eta)\\+g'_{m-i-i}(\eta)\sum_{j=0}^{i}k'_{i-j}(\eta)k''_j(\eta)\\+\frac{1}{\alpha}\left(\begin{array}{l}h'_{m-i-i}(\eta)\sum_{j=0}^{i}f''_{i-j}(\eta)k''_j(\eta)+k'_{m-i-i}(\eta)\sum_{j=0}^{i}f''_{i-j}(\eta)h''_j(\eta)\\+h'_{m-i-i}(\eta)\sum_{j=0}^{i}k'_{i-j}(\eta)f'''_j(\eta)-\frac{M}{\alpha}h_{m-i-i}(\eta)\sum_{j=0}^{i}k_{i-j}(\eta)f''_j(\eta)\end{array}\right)\end{array}\right)\end{array}\right) \quad (48)$$

$$R_{3,m}(\eta)=k''_{m-1}(\eta)(1+\lambda)-Mk_{m-1}(\eta)+\lambda Mk_{m-1}(\eta)+\sum_{i=0}^{m-1}\left(\begin{array}{l}2f_i(\eta)k'_{m-1-i}(\eta)-k_i(\eta)f'_{m-1-i}(\eta)\\+\alpha\ h_i(\eta)g_{m-1-i}(\eta)\end{array}\right)$$

$$-\lambda\sum_{i=0}^{m-1}\left(\begin{array}{l}\xi^2\left(\begin{array}{l}\frac{2}{3}\alpha\ g'_{m-1-i}(\eta)\sum_{j=0}^{i}h'_{i-j}(\eta)f'_j(\eta)+\frac{14}{3}\ f'_{m-1-i}(\eta)\sum_{j=0}^{i}k'_{i-j}(\eta)f''_j(\eta)\\+2\,k''_{m-1-i}(\eta)\sum_{j=0}^{i}f'_{i-j}(\eta)f'_j(\eta)-2Mf'_{m-1-i}(\eta)\sum_{j=0}^{i}k_{i-j}(\eta)f'_j(\eta)\end{array}\right)\\+\gamma\left(\begin{array}{l}h'_{m-1-i}(\eta)\sum_{j=0}^{i}k'_{i-j}(\eta)h''_j(\eta)+\frac{1}{2}k''_{m-1-i}(\eta)\sum_{j=0}^{i}h'_{i-j}(\eta)h'_j(\eta)\\+\frac{3}{2}k''_{m-1-i}(\eta)\sum_{j=0}^{i}k'_{i-j}(\eta)k'_j(\eta)-\frac{M}{2}k'_{m-1-i}(\eta)\sum_{j=0}^{i}k'_{i-j}(\eta)k_j(\eta)\\-\frac{M}{2}h'_{m-1-i}(\eta)\sum_{j=0}^{i}h'_{i-j}(\eta)k_j(\eta)\end{array}\right)\end{array}\right) \quad (49)$$

$$R_{4,m}(\eta)=h''_{m-1}(\eta)(1+\lambda)-Mh_{m-1}(\eta)-\lambda Mh_{m-1}(\eta)+\sum_{i=0}^{m-1}\begin{pmatrix}2f_i(\eta)h'_{m-1-i}(\eta)-h_i(\eta)f'_{m-1-i}(\eta)\\-\alpha\, k_i(\eta)g_{m-1-i}(\eta)\end{pmatrix}$$

$$-\lambda\sum_{i=0}^{m-1}\left(\begin{array}{l}\xi^2\left(\begin{array}{l}\frac{14}{3}f'_{m-i-i}(\eta)\sum_{j=0}^{i}h'_{i-j}(\eta)f'_j(\eta)-\frac{2}{3}\alpha\, g'_{m-i-i}(\eta)\sum_{j=0}^{i}k'_{i-j}(\eta)f'_j(\eta)\\+2h''_{m-i-i}(\eta)\sum_{j=0}^{i}f'_{i-j}(\eta)f'_j(\eta)-2Mf'_{m-1-i}(\eta)\sum_{j=0}^{i}h_{i-j}(\eta)f'_j(\eta)\end{array}\right)\\+\gamma\left(\begin{array}{l}\frac{3}{2}h''_{m-i-i}(\eta)\sum_{j=0}^{i}h'_{i-j}(\eta)h'_j(\eta)+\frac{1}{2}h''_{m-i-i}(\eta)\sum_{j=0}^{i}k'_{i-j}(\eta)k'_j(\eta)\\+h'_{m-i-i}(\eta)\sum_{j=0}^{i}k'_{i-j}(\eta)k''_j(\eta)-\frac{M}{2}h'_{m-1-i}(\eta)\sum_{j=0}^{i}h'_{i-j}(\eta)h_j(\eta)\\-\frac{M}{2}k'_{m-1-i}(\eta)\sum_{j=0}^{i}k'_{i-j}(\eta)k_j(\eta)\end{array}\right)\end{array}\right) \tag{50}$$

and

$$\chi_m=\begin{cases}0, & m\le 1\\1, & m\ge 2\end{cases}$$

By the above process of HAM defined above, it is quite easy to calculate the set of linear Eqs. (42)-(45), one after the other in the order m, particularly by any computational software. Here we computed our calculations with the help of MATHEMATICA 10.

5. Results and discussion

5.1 Flow analysis:

The present study has been made to observe the influence of roational parameter α, fluid parameters $(\lambda,\xi \text{ and } \gamma)$ of Powell Eyring fluid, suction/injection parameter V_0 and porosity parameter on radial velocity function $f'(\eta)$, azimuthal velocity function $g(\eta)$ and on induced velocity function $k(\eta)$ and $h(\eta)$.

Fig. 1 demonstrates the effect of radial parameter α at various values. The increasing values of α shows the increasing effect on radial velocity profile $f'(\eta)$. All the values of α converges to 1, due to the boundary condition of Eq. (15). Fig. 2 shows the combine effect of fluid parameters γ and λ on velocity function $f'(\eta)$, it clearly observed that the influence of fluid parameter γ on $f'(\eta)$ expresses the slow increasing effect as compare to rotational parameter α whereas λ initially shows the deceleration on $f'(\eta)$ near the disk and after the point 2.4 it start accelerating. In Fig. 3 fluid parameters ξ display the decreasing effect on velocity component $f'(\eta)$. The porosity parameter M also expresses the decreasing effect whereas suction/injection parameter shows the acceleration on $f'(\eta)$ just like rotational parameter α (see Fig 4 and 5).

The influence of parameters $\alpha,\gamma,\lambda,\xi,M$ and V_0 on azimuthal velocity profile $g(\eta)$ can be observed from Figs. 6-10. It can be clearly monitor from Fig. 6 that the roational parameter α expresses the deceleration on azimuthal velocity function $g(\eta)$. Same as roational parameter α, fluid parameters λ and γ also shows the deceleration on increasing values. As comppare to α the decreasing rate of λ and γ is slow (see Fig 7). In Fig. 8 the fluid parameter ξ intimate quite different effect as compare to other parameters, it first illustrate the acceleration effect and after the point 1.2 it start decelerating on azimuthal velocity $g(\eta)$. Figs 9 and 10 depicted the impact of porosity paramter and suction/injection paratmeter, both expresses the decline on increasing values.

Figs. 11-15 explicate the outcome of parameters $\alpha, \gamma, \lambda, \xi, M$ and V_0 on induced velocity function $k(\eta)$. Parameter α and γ express the similar behaviour, they manifest the speeding up in velocity $k(\eta)$ on increasing values of parameters (see Fig 11 and 12). If we observe closely boht the Figs we can see that the behabiour of induced velocity function $k(\eta)$ is same but α accelerates rapidly as compare to γ on increasing values of parameters. The non-dimensional parameter γ accelerates on high values, but on small values it doesn't show any impact on $k(\eta)$. Fig. 12 also examine the impact of parameter λ on $k(\eta)$ exponential decline near the disk and then starts rising from point 2.4. The fluid parameter ξ is a decline function of induced velocity component $k(\eta)$(see Fig. 13). In Fig. 14 porosity parameter displays both type of effects, decreasing near the disk and after certain point it shows acceleration. The influence of Suction/Injection parameter V_0 is observed in Fig. 15 which determine the fall off on velocity component $k(\eta)$.

The impacts of induced velocity function $h(\eta)$ perceived on different values of paramters are described in Fig 16-20. It can be seen from Fig. 16 that the rotational parameter α deceleretes the induced velocity component $h(\eta)$. Non dimensional paramter γ shows the creaping decline impact on $h(\eta)$ whereas fluid parameter λ displays the positive impact on the induced velocity $h(\eta)$ (see Fig. 17). Fig 18 appears both positive and negative effect of ξ on $h(\eta)$, first it display the positive effect near the disk and after reaching the point 1.4 it start showing the negative effect on velocity component $h(\eta)$. The influence of porosity parameter M and Suction/Injection parameter is investigated in Fig. 19 and 20 which demonstrates the negative impact on velocity $h(\eta)$.

5.2 Convergence analysis:

The Fig. 21 exhibit the convergence region of $\hbar-$curve for the velocity functions $f''(0)$, $g'(0)$, $k'(0)$ and $h'(0)$.It can be easily seen that the valid range for the values of $\hbar_1, \hbar_2, \hbar_3$ and $\hbar_4$ are $-1.0 < \hbar_1 < 1.0$, $-1.0 < \hbar_2 < 0.5$, $-1.2 < \hbar_3 < 1.4$, $-1.6 < \hbar_4 < 0.8$.

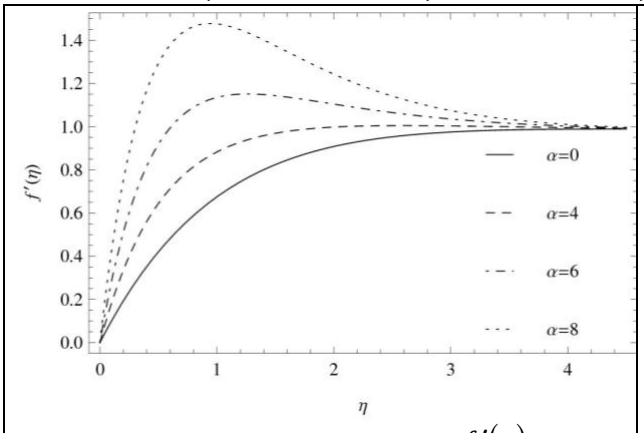

Fig. 1: The Effect of α on velocity profile $f'(\eta)$ at $\lambda = 0.1,\ \xi = 0.1,\ \gamma = 0.1,\ M = 0.1,\ V_0 = 0.1$ and $\hbar = -0.05$

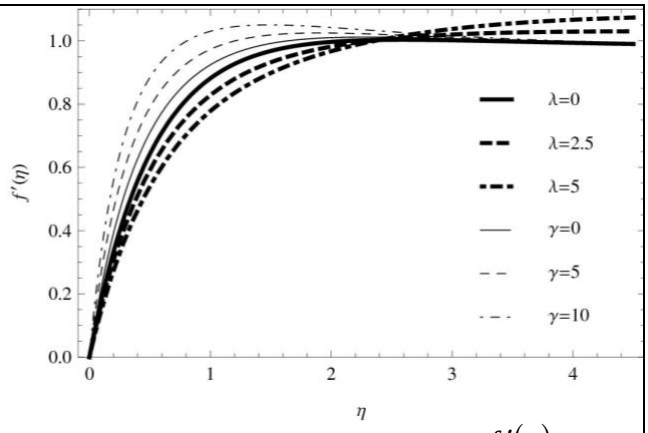

Fig. 2: The Effect of γ and λ on velocity profile $f'(\eta)$ at $\lambda = 0.1, \xi = 0.1, \alpha = 4, M = 0.1,\ V_0 = 0.1$ and $\hbar = -0.05$

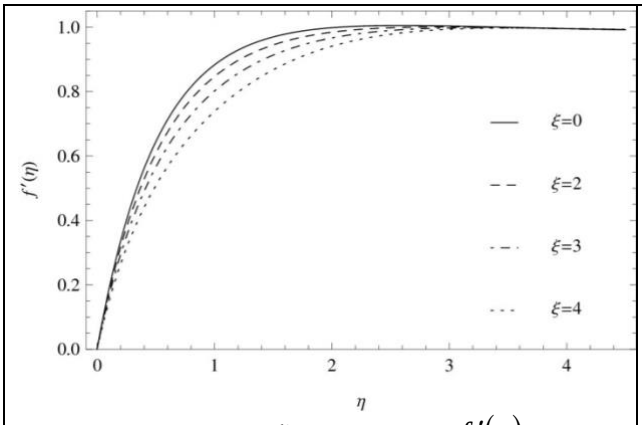

Fig. 3: The Effect of ξ on velocity profile $f'(\eta)$ at
$\alpha = 4, \lambda = 0.1, \gamma = 0.1,\ M = 0.1,\ V_0 = 0.1$ and $\hbar = -0.05$

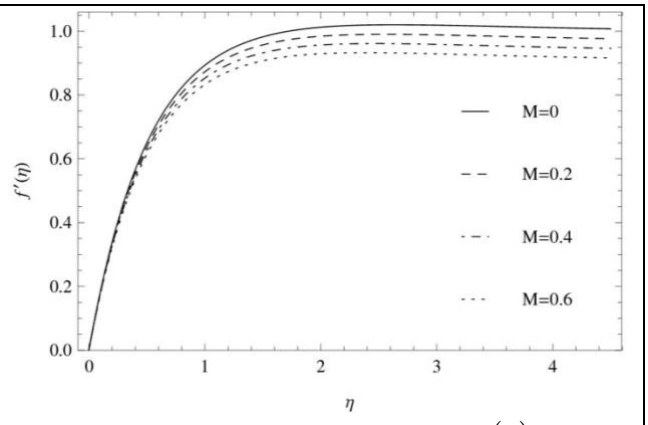

Fig. 4: The Effect of M on velocity profile $f'(\eta)$ at
$\alpha = 4, \lambda = 0.1, \gamma = 0.1,\ \xi = 0.1,\ V_0 = 0.1$ and $\hbar = -0.05$

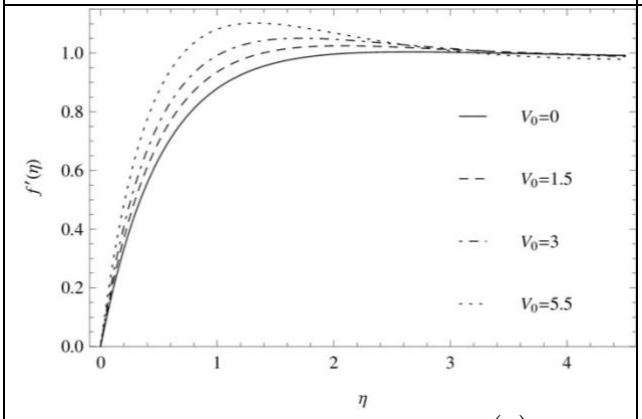

Fig. 5: The Effect of V_0 on velocity profile $f'(\eta)$ at
$\alpha = 4, \lambda = 0.1, \gamma = 0.1,\ \xi = 0.1,\ \mathrm{M} = 0.1$ and $\hbar = -0.05$

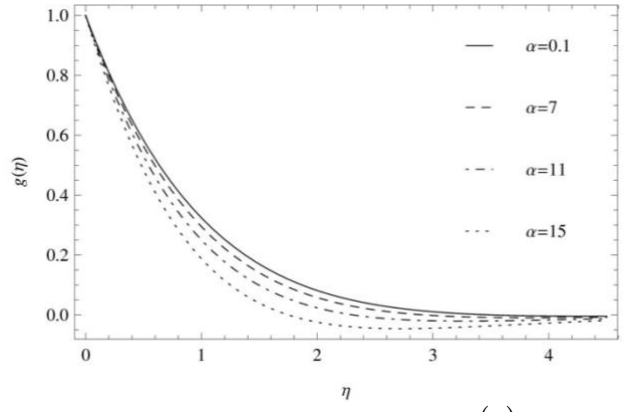

Fig. 6: The Effect of α on velocity profile $g(\eta)$ at
$\lambda = 0.1,\ \xi = 0.1,\ \gamma = 0.1,\ M = 0.1,\ V_0 = 0.1$ and $\hbar = -0.05$

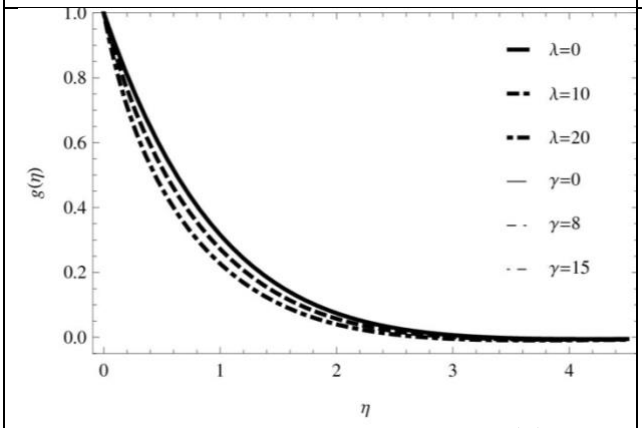

Fig. 7: The Effect of γ and λ on velocity profile $g(\eta)$ at
$\lambda = 0.1, \xi = 0.1, \alpha = 4, M = 0.1,\ V_0 = 0.1$ and $\hbar = -0.05$

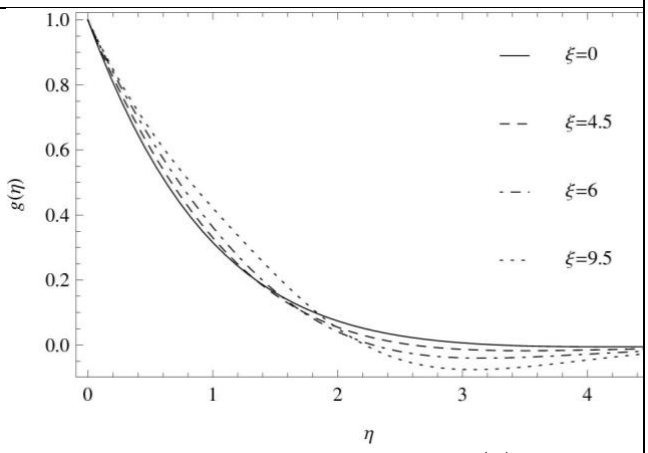

Fig. 8: The Effect of ξ on velocity profile $g(\eta)$ at
$\alpha = 4, \lambda = 0.1, \gamma = 0.1,\ M = 0.1,\ V_0 = 0.1$ and $\hbar = -0.05$

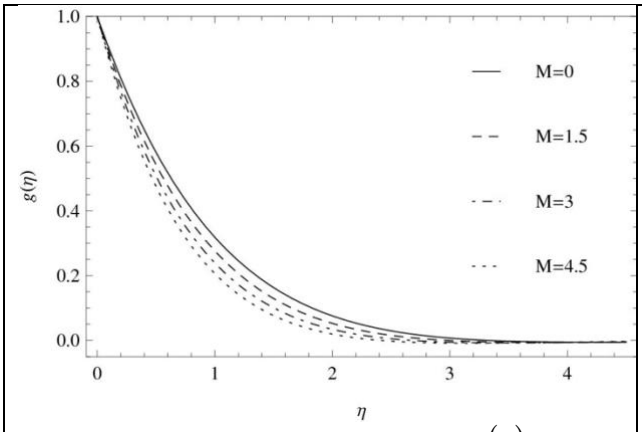

Fig. 9: The Effect of M on velocity profile $g(\eta)$ at
$\alpha = 4, \lambda = 0.1, \gamma = 0.1,\ \xi = 0.1,\ V_0 = 0.1$ and $\hbar = -0.05$

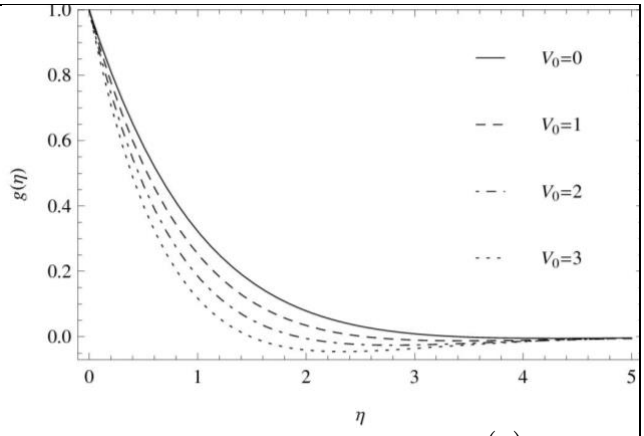

Fig. 10: The Effect of V_0 on velocity profile $g(\eta)$ at
$\alpha = 4, \lambda = 0.1, \gamma = 0.1,\ \xi = 0.1,\ \mathrm{M} = 0.1$ and $\hbar = -0.05$

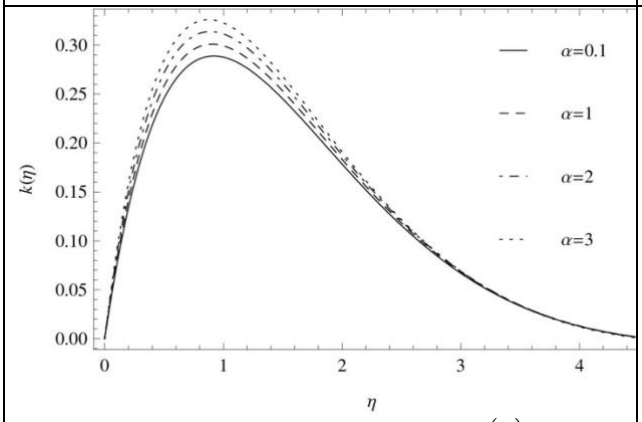

Fig. 11: The Effect of α on velocity profile $k(\eta)$ at
$\lambda = 0.1,\ \xi = 0.1,\ \gamma = 0.1,\ M = 0.1,\ V_0 = 0.1$ and $\hbar = -0.05$

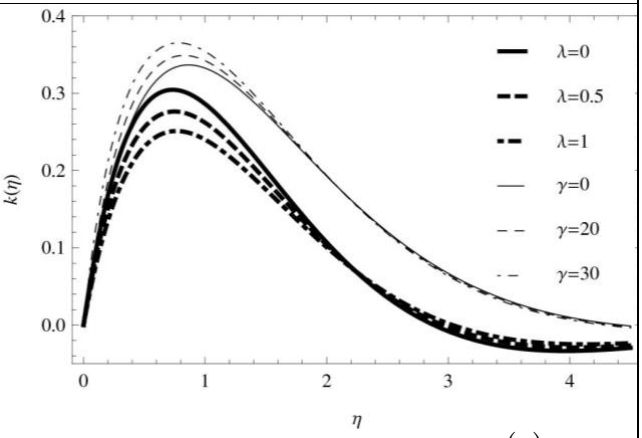

Fig. 12: The Effect of γ and λ on velocity profile $k(\eta)$ at
$\lambda = 0.1, \xi = 0.1, \alpha = 4, M = 0.1,\ V_0 = 0.1$ and $\hbar = -0.05$

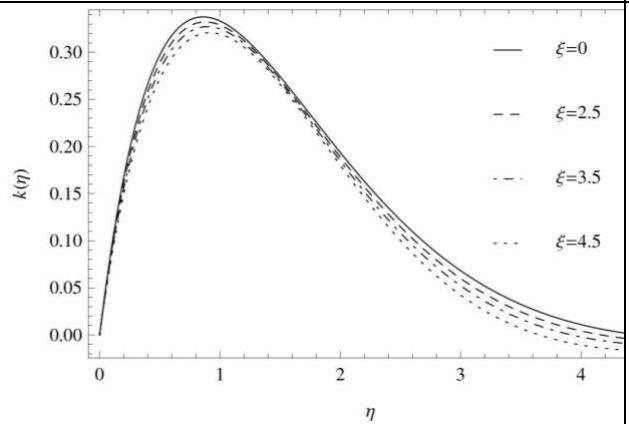

Fig. 13: The Effect of ξ on velocity profile $k(\eta)$ at
$\alpha = 4, \lambda = 0.1, \gamma = 0.1,\ M = 0.1,\ V_0 = 0.1$ and $\hbar = -0.05$

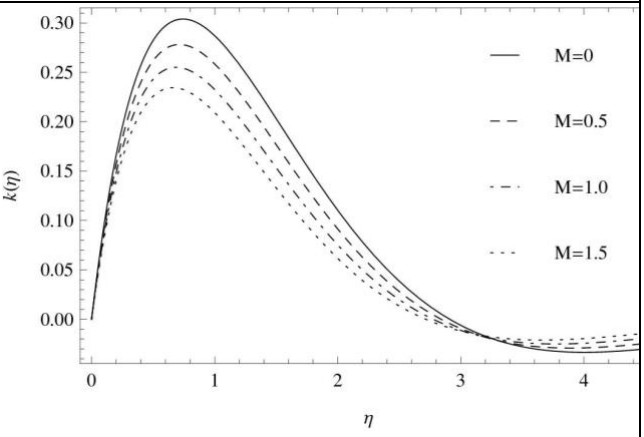

Fig. 14: The Effect of M on velocity profile $k(\eta)$ at
$\alpha = 4, \lambda = 0.1, \gamma = 0.1,\ \xi = 0.1,\ V_0 = 0.1$ and $\hbar = -0.05$

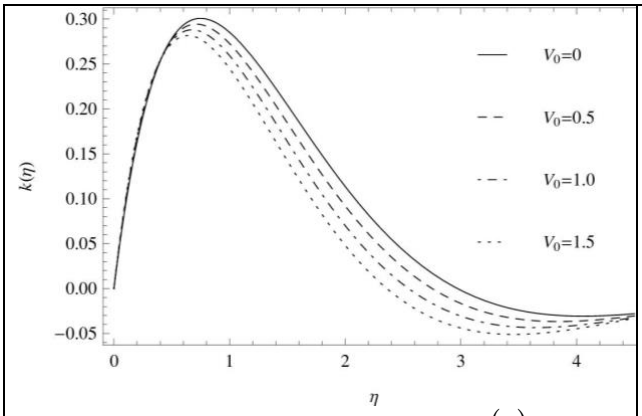

Fig. 15: The Effect of V_0 on velocity profile $k(\eta)$ at
$\alpha = 4, \lambda = 0.1, \gamma = 0.1,\ \xi = 0.1,\ \mathrm{M} = 0.1$ and $\hbar = -0.05$

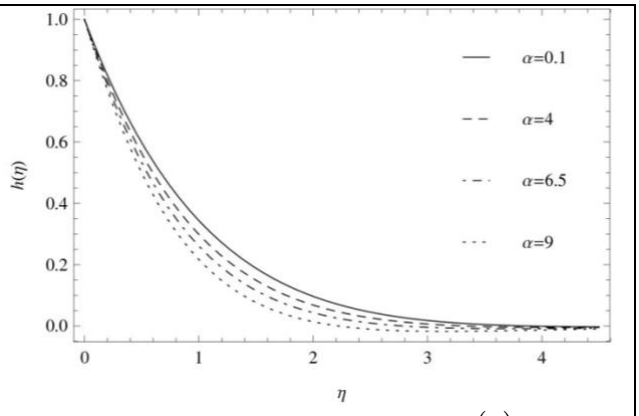

Fig. 16: The Effect of α on velocity profile $h(\eta)$ at
$\lambda = 0.1,\ \xi = 0.1,\ \gamma = 0.1,\ M = 0.1,\ V_0 = 0.1$ and $\hbar = -0.05$

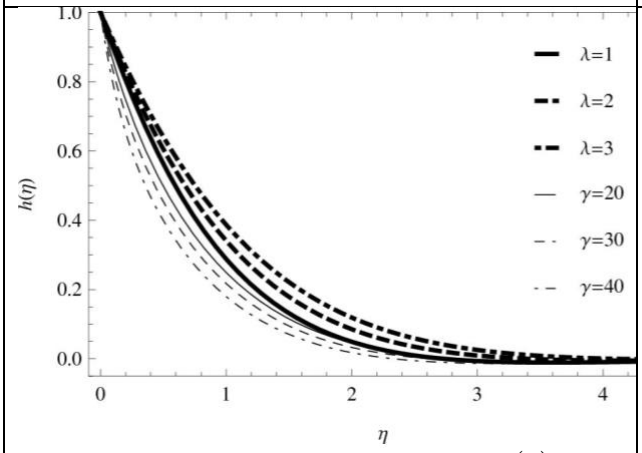

Fig. 17: The Effect of γ and λ on velocity profile $h(\eta)$ at
$\lambda = 0.1, \xi = 0.1, \alpha = 4, M = 0.1,\ V_0 = 0.1$ and $\hbar = -0.05$

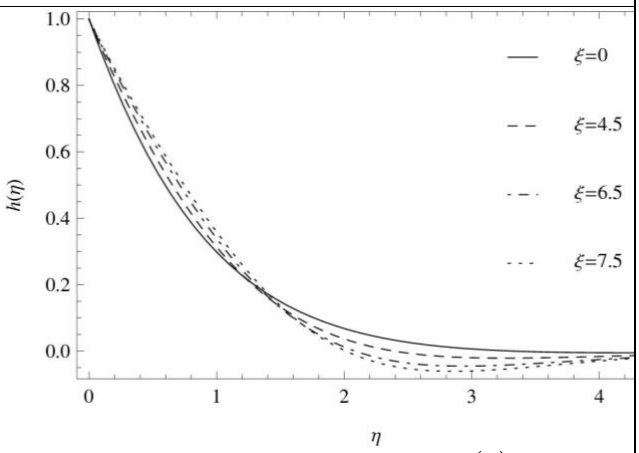

Fig. 18: The Effect of ξ on velocity profile $h(\eta)$ at
$\alpha = 4, \lambda = 0.1, \gamma = 0.1,\ M = 0.1,\ V_0 = 0.1$ and $\hbar = -0.05$

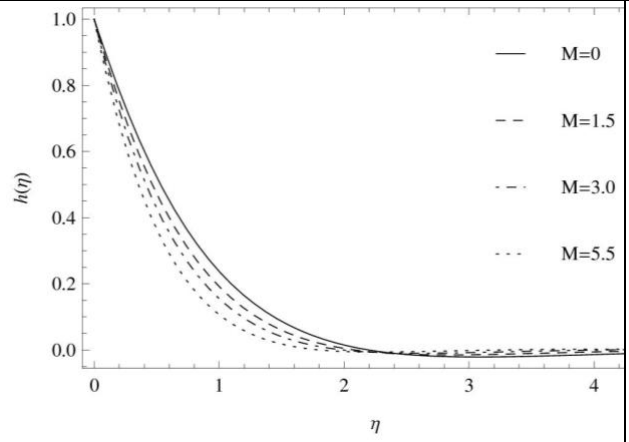

Fig. 19: The Effect of M on velocity profile $h(\eta)$ at
$\alpha = 4, \lambda = 0.1, \gamma = 0.1,\ \xi = 0.1,\ V_0 = 0.1$ and $\hbar = -0.05$

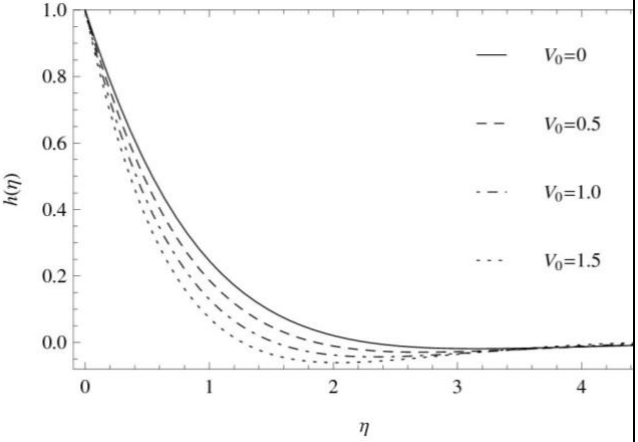

Fig. 20: The Effect of V_0 on velocity profile $h(\eta)$ at
$\alpha = 4, \lambda = 0.1, \gamma = 0.1,\ \xi = 0.1,\ \mathrm{M} = 0.1$ and $\hbar = -0.05$

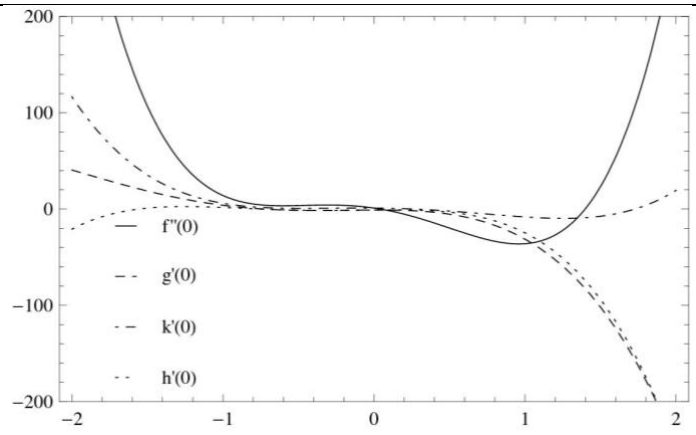

Fig. 21: The $\hbar$ of $f''(0),\ g'(0),\ k'(0)$ and $h'(0)$

6. Conclusion

In this present study the nonlinear problem, the off centered stagnation flow of a three-dimensional Powell-Eyring fluid towards a rotating porous disk. The non perturbation method HAM is used to calculate the analytical solutions of the governing ordinary differential equation system. The impact of the parameters is examined on the radial, azimuthal and induced velocity function. The flow analysis has been made by graphical form. The main outcomes are summarized as follows.

- The impact of $\alpha,\ V_0$ and γ express the acceleration on the velocity function f'.
- The influence of fluid parameter ξ exhibits the decline effect on velocity function f'.
- The porosity parameter displays the negative impact on velocity function f'.
- The variations of parameter, α , $\gamma,\ M, V_0$ and λ are qualitatively similar on the velocity function g.
- The non dimensional parameters α and γ shows similar increasing effect on k.
- The parameter λ gives exponential decrease near the disk and then starts accelerating on the velocity function k.
- The Suction/Injection parameter shows the negative influence on the velocity function k.
- $\alpha,\ M,\ V_0$ and γ demonstrate the fall on the velocity function h, whereas λ presented the rise on the velocity function h.
- The fluid parameter ξ shows both positive and negative behavior on velocity function h.

References

[1] R.V. Williamson, The flow of pseudo plastic materials, Industrial & Engineering Chemistry Research, 21(11) (1929), 1108-1111.
[2] R.E. Powell, H. Eyring, Mechanisms for the relaxation theory of viscosity, Nature, 154 (1944), 427–428.
[3] V.K. Stokes, Couple stresses in fluids, Physics Fluids, 9 (1966), 1709–1715.
[4] E.C. Bingham, An Investigation of the Laws of Plastic Flow, U.S. Bureau of Standards Bulletin, 13 (1916), 309-353.
[5] N. Casson, Rheology of disperse systems, in Flow Equation for Pigment Oil Suspensions of the Printing Ink Type, Rheology of Disperse Systems, C. C. Mill, Ed., Pergamon Press, London, UK, (1959), 84–102.
[6] T. Hayat, M. Pakdemirli, Y. Aksoy, similarity solutions for boundary layer equations of a Powell-Eyring fluid, Mathematical and Computational Application, 18(1) (2013), 62-70.
[7] S. Islam, A. Shah, C.Y. Zhou, I. Ali, Homotopy perturbation analysis of slider bearing with Eyring-Powell fluid, Z. Angew. Math. Physics, 60 (2009), 1178–1193.
[8] J. Zueco, O.A. Beg, Network numerical simulation applied to pulsatile non-Newtonian flow through a channel with couple stress and wall mass effects, International Journal of Applied Mathematics, 5 (2009), 1-16.

[9] M. Patel, M.G. Timol, Numerical treatment of Eyring- Powell fluid flow using method of asymptotic boundary conditions, Applied Numerical Mathematics, 59 (2009), 2584–2592.
[10] T. Javed, N. Ali, Z. Abbas, M. Sajid, Flow of an Erying-Powell non-Newtonian fluid over a stretching sheet, Chemical Engineering Communications, 200 (2013), 327–336.
[11] N.S. Akbar, S. Nadeem, Characteristics of heating scheme and mass transfer on the peristaltic flow for an Eyring-Powell fluid in an endoscope, International Journal of Heat and Mass Transfer, 55 (2012), 375–383.
[12] T. Hayat, Z. Iqbal , M. Qasim, S. Obaidat, Steady flow of an Eyring Powell fluid over a moving surface with convective boundary conditions, Journal of Heat and Mass Transfer, 55 (2012), 1817–1822.
[13] T. Von Kármán, Uber laminare und turbulente Reibung, Zeitschrift für Angewandte Mathematik und Mechanik, 1(4) (1921), 233–252.
[14] K. Millsaps, Heat transfer by laminar flow from a rotating plate, Journal of Aeronautical Sciences, 18(5) (1951), 354-355.
[15] A. Ahmadpour, K. Sadeghy, Swirling flow of Bingham fluids above a rotating disk: An exact solution, Journal of Non-Newtonian Fluid Mechanics, 197 (2013), 41-47.
[16] M.M. Rashidi, H. Shahmohamadi, analytical solution of three dimensional Navier-strokes equation for the flow near an infinite rotating disk, Communications in Nonlinear Science and Numerical Simulation, 14(7) (2009), 2999-3006.
[17] N.A. Khan, S. Aziz, Nadeem Alam Khan, MHD flow of Powell–Eyring fluid over a rotating disk, Journal of the Taiwan Institute of Chemical Engineers, 45 (2014), 2859–2867.
[18] P. Ram , A. Bhandari, Effect of phase difference between highly oscillating magnetic field and magnetization on the unsteady ferro fluid flow due to a rotating disk, Results in Physics, 3 (2013), 55–60.
[19] C.Y. Wang, Nonaligned stagnation flow towards a rotating disk, International Journal of Engineering Science, 46 (2008), 391-396.
[20] S. Dinarvand, On explicit, purely analytic solutions of nonaligned stagnation flow towards a rotating disk by means of HAM, Nonlinear Analysis; RWA 11(5) (2010), 3389-3398.
[21] E. Erfani, M.M. Rashidi, A.B. Parsa, The modified differential transform method for solving off-centered stagnation flow toward a rotating disc, International Journal of Computational Methods,7 (4) (2010), 655-670.
[22] S.H. Nourbakhsh, A.A. Pasha Zanoosi, A.R. Shateri, Analytical solution for off-centered stagnation flow towards a rotating disc problem by homotopy analysis method with two auxiliary parameters, Communications in Nonlinear Science and Numerical Simulation, 16 (7) (2011), 2772–2787.
[23] N.A. Khan, S. Khan, F. Riaz, Analytic Approximate Solutions and Numerical Results for Stagnation Point Flow of Jeffrey Fluid Towards an Off-Centered Rotating Disk, Journal of Mechanics, (2014) 1-15.
[24] N.A. Khan, F. Riaz, Off-centered stagnation point flow of a couple stress fluid towards a Rotating Disk, The Scientific World Journal, 2014, (2014), Article ID 163586.
[25] F. Shahzad, T. Hayat, O.M. Aldossary, Oscillatory flow of fourth order fluid in a porous half space, Chemical Engineering Communications, 199, (2012) 1072-1084.
[26] W.C. Tan, T. Mausoka, Stokes' first problem for a second grade fluid in a porous half space with heated boundary, International Journal of Non-Linear Mechanics, 40 (2005), 515-522.
[27] W.C. Tan, T. Mausoka, Stokes' first problem for an Oldryod-B fluid in a porous half space, Physics of Fluids, 17 (2005), 023101-023107.
[28] T. Hayat, C. Fetecau, M. Sajid, On MHD transient flow of a Maxwell fluid in a porous medium and rotating frame, Physics Letters A 372 (2008), 1639-1644.
[29] H.A. Attia, Rotating disk flow and heat transfer through a porous medium of a non-Newtonian fluid with suction and injection, Communications in Nonlinear Science and Numerical Simulation, 13 (2008), 1571–1580.
[30] H.A. Attia, Unsteady flow and heat transfer of viscous incompressible fluid with temperature-dependent viscosity due to a rotating disk in a porous medium, Journal of Physics A: Math Gen 39(4) (2006), 979–91.